

ESTIMATING THE MAIN RADIATION SOURCE TERMS FOR THE NICA COLLIDER

*M. Paraipan, G. N. Timoshenko*¹

Joint Institute for Nuclear Research, Dubna

Various radiation sources at the NICA collider were identified and specified. It is found that the most powerful ones are the beam catchers restricting the beam «halo». The double differential neutron yields from the catcher are calculated using the GEANT4 code. A simulation of the total absorbed dose in the magnet superconducting winding due to the catcher radiation is carried out for the accepted levels of beam losses. The induced radioactivity of the catcher is predicted for the collider schedule.

Даны описание и характеристики различных источников вторичного излучения коллайдера NICA. Наиболее значимыми источниками являются перехватчики ионов, органичивающие «гало» пучков. С помощью программы GEANT4 были рассчитаны двойные дифференциальные выходы нейтронов из перехватчиков. Оценки показали, что поглощенная доза в обмотках сверхпроводящих магнитов, обусловленная вторичным излучением из перехватчиков, не превысит допустимого уровня. Выполнен прогноз уровней наведенной активности перехватчиков пучков в соответствии с расписанием работы коллайдера.

PACS: 87.56.bg; 25.75.-q; 61.80.-x

The NICA collider is designed at the Joint Institute for Nuclear Research for ion–ion (¹⁹⁷Au) and ion–proton beams collisions in the kinetic energy range 1–4.5 GeV/nucleon and also for polarized proton–proton (5–12.6 GeV) and deuteron–deuteron (2–5.8 GeV/nucleon) collisions. The collider will have the racetrack shape with two arcs and two long straight parts. The total collider perimeter will be 503 m. The collider rings will have two interaction points with particle detectors located in the straight parts of the collider. The most hard radiation situation at the collider will be in the mode of ion–ion collision. The beam intensity will be about 10¹¹ ions in each collider ring distributed over 22 bunches. The main radiation sources at the collider will be the following:

- 1) beam injection devices (septum kicker magnets);
- 2) residual gas within the ion pipes;
- 3) beams «halo» losses restricted by the beam catchers;
- 4) recombination of ions with electrons from the beam cooling system.

All these sources are emitters of high-energy hadrons. Besides, there is a powerful gamma-ray source: the system of the electron cooling of the ion beams.

The radiation sources mentioned in the first item of the list above will be located in two places of the short straight section in the arcs. The second source will be uniformly distributed

¹E-mail: tim@jinr.ru

along the collider rings and is not significant in comparison with the other sources. The third source is related to intra-beam scattering due to the beta-function and dispersion variations. The FODO-cell (11.96 m) was chosen for the collider optics (12 cells per arc). In order to restrict the beam «halo» within the finite aperture, several beam catchers are usually mounted in the ring. The catchers are powerful local radiation sources. The fourth source is associated with ion charge change and recombined ions leaving the beam. These ion losses will also take place in the catchers.

Two versions of the beam catcher design for the NICA collider were considered. The first is a thick heterogeneous catcher for the absorption of the main part of primary-ion energy to provide the radiation shielding of the consecutive magnet optic element. It consists of the initial part made of graphite and the one-meter-long second part made of steel. But the catcher's great length does not allow mounting them in the collider arcs, where the beam emittance variations are the largest. The second version of the beam catcher is intended for stopping only the primary ions without suppressing secondary radiation. The thickness of the small steel catcher is 130 mm; its cross section is 160×130 mm. It is planned to mount in tens of catchers in every ring within the periodic optic structure of every arc (at the beam dispersion function maxima [1]), and the catchers will be arranged in twos in each straight part of the collider (48 catchers in total). The catchers in both rings are stacked. The collider scheme with the disposition of the main radiation sources is shown in Fig. 1.

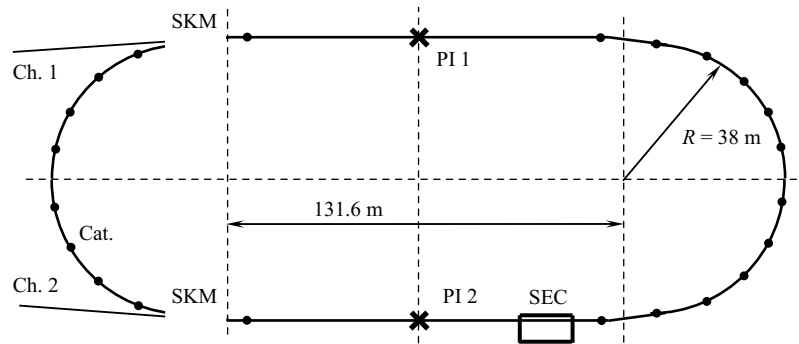


Fig. 1. The disposition of the main radiation sources at the NICA collider. Ch. 1, 2 — beam transport channels; SKM — septum kicker magnets; SEC — system of electron cooling; PI 1, 2 — points of interaction. The bold points at the collider rings denote the beam catchers

The beam losses at each septum kicker magnet are supposed to be $5 \cdot 10^6 \text{ s}^{-1}$. The residual gas-related ion losses, which are uniformly distributed along the collider perimeter, are assumed to be 10^5 s^{-1} . The maximum «halo» losses in each catcher are assumed to be 10^7 s^{-1} . The total recombined ion losses are supposed to be $5 \cdot 10^7 \text{ s}^{-1}$ in each ring. These losses can occur in the first several catchers downstream the beam. All the loss values are estimated with a reserve coefficient of 2 for radiation protection purposes.

The collider schedule will be the following: 22 hours of work and a two-hour maintenance break between the runs; 8 continuous months of work and a four-month dwell per year; the total duration of work is planned to be 10 years.

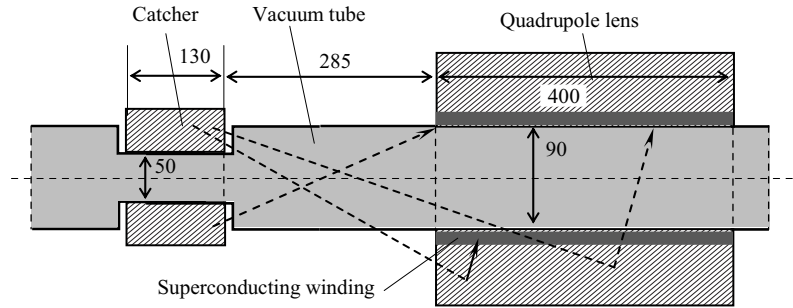


Fig. 2. The geometry of superconducting winding irradiation by secondary hadrons from the catcher

The beam catcher source term is the most important for the estimation of both radiation shielding and superconductor quench probability. The secondary hadron radiation from the beam catcher will determine the irradiation of the radiation-nonresistant structural elements such as superconducting cables and insulating materials of the quadrupole lens and dipole magnet. The irradiation of the quadrupole lens, which is arranged directly downstream the catcher, was simulated with the GEANT4 code [2, 3] in the rough geometry presented in Fig. 2. The vacuum tube cross section within the catcher is assumed to be round (rather than elliptical) with an equivalent diameter of 50 mm. The steel yoke of the magnet is 400 mm in length; the vacuum tube cross section inside it is also assumed to be round with a diameter of 90 mm. Since the average density of the superconducting cable is close to that of steel, the detailed geometry of the superconducting winding was not taken into account. The lens winding with a superconducting cable was imitated by a steel layer (as part of the yoke), but with an equivalent density of $7 \text{ g} \cdot \text{cm}^{-3}$. The average cross section of the lens yoke is accepted to be $230 \times 230 \text{ mm}$.

The quadrupole lens is irradiated by the forward hadron radiation from the catcher (the neutron spectra from the catcher at small degrees are shown in Fig. 3). The catcher thickness is insufficient for internuclear cascade development, and the cascade processes continue in

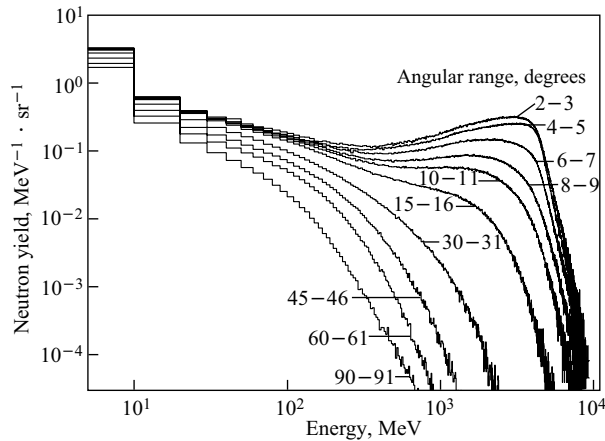


Fig. 3. Double differential neutron yields from the catcher

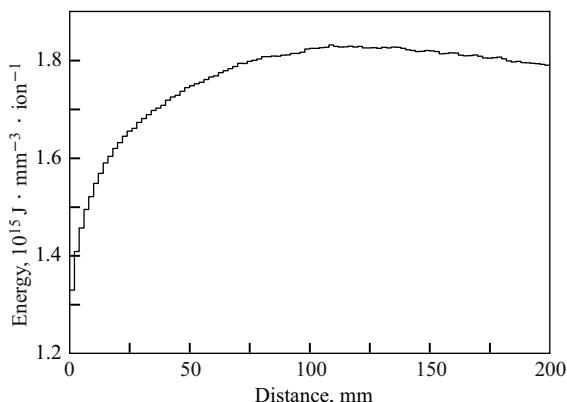


Fig. 4. The spatial distribution of the absorber dose along the superconducting winding

the lens yoke. The spatial distribution of the absorbed dose along the narrow layer of steel imitating the superconducting cable is presented in Fig. 4. The maximum of specific energy deposition in the superconducting layer is observed at 110 mm from the front side of the lens — $1.83 \cdot 10^{-15} \text{ J} \cdot \text{mm}^{-3}$ per ion hitting the catcher or $2.61 \cdot 10^{-3} \text{ mJ} \cdot \text{g}^{-1} \cdot \text{s}^{-1}$ at a catcher beam loss rate of 10^7 s^{-1} .

For a Nuclotron-type magnet, tolerable energy deposition in the superconducting winding (the quench limit) is about $1.65 \text{ mJ} \cdot \text{g}^{-1}$ (adiabatic) and $14 \text{ mW} \cdot \text{g}^{-1}$ (continuous) [4]. It corresponds to $14 \text{ mJ} \cdot \text{g}^{-1} \cdot \text{s}^{-1}$ for permanent irradiation, i.e., is much greater than real energy deposition.

At a beam loss rate of 10^7 s^{-1} in the catcher and with the accepted time schedule, the total absorbed dose for the superconducting cable related to the catcher radiation will be less than $5 \cdot 10^5 \text{ Gy}$. For a Nb–Ti superconducting cable in a Nuclotron-type magnet, the lifetime dose limit is accepted to be $5 \cdot 10^6 \text{ Gy}$ [5]. The radiation hardness of organic materials is even lower than for superconducting materials: about 10^6 Gy .

The contributions of the initial ions lost owing to the residual gas ($2 \cdot 10^2 \text{ s}^{-1}$ per running meter of the ring) to the absorbed dose for the superconducting cable and to the induced activities were estimated to be negligibly small in comparison with the catcher effect. The angles of the ion loss emission from the beam used for the calculation were within the statistical sampling of $0-1^\circ$.

The recombination of the beam ions with cooling system electrons can result in an increase in the ion loss rate in the first several catchers up to $2 \cdot 10^7 \text{ s}^{-1}$. It would be acceptable for the superconducting cable but hazardous for the organic materials. Though, taking into account the conservatism of our estimations, it can be expected that the radiation hardness of both superconducting and organic materials will not be overlapped to the end of the collider work.

Another important feature of the steel catcher is the high level of induced radioactivity due to the maximum ion loss rate. The evolution of the total residual activity of the catcher's steel at the ion loss rate of 10^7 s^{-1} is shown in Fig. 5 for one month and for ten years. According to our estimation, the total specific activity in the catcher at the end of the collider operation will be no more than $3.3 \cdot 10^7 \text{ Bq} \cdot \text{kg}^{-1}$ to the end of irradiation and approximately $2.5 \cdot 10^7 \text{ Bq} \cdot \text{kg}^{-1}$ two hours later. It should be noted that the total specific activity of steel has increased 3.3-fold in as long as ten years owing to long-lived radionuclides.

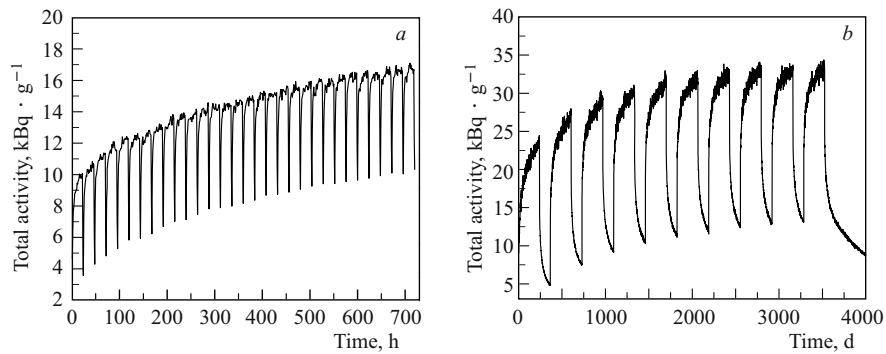


Fig. 5. The evolution of the total residual activity of the catcher's steel during the first month (a) and to the end of the collider operation (b)

Besides the total specific activity of the catcher, the partial specific activities of middle and long-lived radionuclides were predicted. The results of one-month and ten-year predictions are presented in table. The permissible levels of radionuclide specific activity above which the

Predicted levels of induced radioactivity at the catcher. The bold font and shadow background denote the excess of the permissible levels for nonwaste materials

Isotope	Partial specific activity after 1 month, $\text{Bq} \cdot \text{kg}^{-1}$	Partial specific activity after 10 years, $\text{Bq} \cdot \text{kg}^{-1}$	Permissible specific activity for nonwaste materials, $\text{Bq} \cdot \text{kg}^{-1}$ [5]
^{35}S	$1.4 \cdot 10^4$	$2.45 \cdot 10^4$	10^5
^{38}Cl	$1.15 \cdot 10^4$	$1.17 \cdot 10^4$	10^4
^{42}K	$1.6 \cdot 10^4$	$1.65 \cdot 10^4$	10^5
^{43}K	$1.14 \cdot 10^5$	$1.15 \cdot 10^5$	10^4
^{45}Ca	$2.3 \cdot 10^3$	$1.1 \cdot 10^4$	10^5
^{47}Ca	$1.8 \cdot 10^3$	$4.2 \cdot 10^3$	10^4
^{46}Sc	$8.2 \cdot 10^3$	$3.8 \cdot 10^4$	10^2
^{47}Sc	$3.3 \cdot 10^4$	$3.3 \cdot 10^4$	10^5
^{48}Sc	$1.4 \cdot 10^4$	$1.4 \cdot 10^4$	10^3
^{48}V	$2.3 \cdot 10^5$	$2.3 \cdot 10^5$	10^3
^{51}Cr	$2.8 \cdot 10^5$	$5.7 \cdot 10^5$	10^5
^{52}Mn	$4.5 \cdot 10^5$	$4.6 \cdot 10^5$	10^3
^{54}Mn	$3.8 \cdot 10^4$	$5.5 \cdot 10^5$	10^2
^{52}Fe	$2.55 \cdot 10^5$	$2.8 \cdot 10^5$	10^4
^{55}Fe	$4.2 \cdot 10^4$	$1.5 \cdot 10^6$	10^6
^{59}Fe	$4.1 \cdot 10^3$	$1.4 \cdot 10^4$	10^3
^{55}Co	$4.9 \cdot 10^4$	$5.3 \cdot 10^4$	10^4
^{56}Co	$2.4 \cdot 10^4$	$7.2 \cdot 10^4$	10^2
^{57}Co	$4.6 \cdot 10^3$	$1.9 \cdot 10^4$	10^3

material becomes radioactive waste are given in [6]. Among the radionuclides with $A \leq 56$ (target fragments predominately and projectile fragments partly), the highest exceedance of the permissible levels are observed for ^{48}V , ^{52}Mn , ^{54}Mn , and ^{56}Co even after a month-long catcher irradiation. The radionuclides with $A > 56$ (projectile fragments exclusively) have very low specific activities. The same will probably be true for the quadrupole lenses exposed to secondary radiation from the catchers due to the extension of internuclear cascade development within the lens.

Our simulation predicts the equivalent dose rate to be less than $10 \mu\text{Sv} \cdot \text{h}^{-1}$ at a distance of 1 m from the catcher after 10 years of work. It means that personnel access to the collider tunnel would be allowed under a special procedure.

REFERENCES

1. *Kostromin S. et al.* Lattice of NICA Collider Rings // Proc. of IPAC'10, Kyoto, Japan, May 23–28, 2010. P. 690–692.
2. *Allison J. et al.* GEANT4 Developments and Applications. IEEE Trans. // Nucl. Sci. 2006. V. 53. P. 270–278.
3. *Agostinelli S. et al.* GEANT4 — a Simulation Toolkit // Nucl. Instr. Meth. A. 2003. V. 506. P. 250–303.
4. *Fischer E. et al.* Design and Development of Superconducting Magnets for the New Accelerator Facilities. GSI Scientific Report 2002 / GSI Report 2003-1. P. 202.
5. *Smirnov A.* The Nuclotron Is a New Technology of the Synchrotron Superconducting Magnet System // Part. Nucl. 2001. V. 32, No. 1. P. 105 (in Russian).
6. Main Sanitary Rules of Radiation Protection Guarantee for Workers and the Public OSPORB-99/2010. Rus. Ministry of Health. M., 2010 (in Russian).

Received on March 2, 2012.